RSC Advances

ROYAL SOCIETY OF CHEMISTRY

www.rsc.org/advances

Effect of L-tyrosine on aerobic sludge granulation and its stability

Jinghai Luo[a], Li Wei[a], Tianwei Hao[a*], Weiqi Xue[a], Hamish R. Mackey[c], Guang-Hao Chen[a,b]

[a]Department of Civil and Environmental Engineering, the Hong Kong University of Science and Technology, Clear Water Bay, Hong Kong, China.

[b]SYSU-HKUST Research Centre for Innovative Environmental Technology, Sun Yat-sen University, Guangzhou, China

[c]College of Science, Engineering and Technology, Hamad bin Khalifa University, Education City, Doha, Qatar

([*]Corresponding author: thao@connect.ust.hk)

Abstract:

Aerobic sludge granulation and its stability remain challenging in application. Tyrosine, a compound in extracellular polymeric substances (EPSs) extracted from sludge, is reported to be closely associated with sludge granulation and its stability. In order to confirm this, this study investigated the effect of L-tyrosine on granulation and disintegration of granular sludge in two identical sequencing airlift bioreactors (SABRs): one dosed with L-tyrosine (6 mg/L) and the other without dosing. Changes in the physiochemical and biological properties of the aerobic granular sludge (AGS) and organic and nitrogen removal in both reactors operated under different ratios of chemical oxygen demand (COD) to nitrogen were closely monitored for 120 days. The L-tyrosine dosing shortened full granulation of AGS by 1 month. Disintegration of the granules and deterioration in the COD and nitrogen removal capability were not observed in the L-tyrosine dosed reactor even when the ratio of COD/N in the influent was reduced from 4 to 1, in order to test AGS disintegration. This clearly confirmed the contribution of L-tyrosine in promoting AGS granulation and its stability. Both

the enrichment of quorum sensing auto-inducer relating bacteria genera (21%) and the stable production of EPS were suggested as main reasons for the positive effect of L-tyrosine on the granulation and stability of AGS.

Keywords: Aerobic granular sludge; granulation and stability; L-tyrosine effect; COD/N ratio

1. Introduction

As a special form of biofilm, aerobic granular sludge (AGS) has been recognized as a low energy and small footprint technology for substituting activated sludge processes for municipal and industrial wastewater treatment.[1] The merits of AGS, including improved settleability, high biomass retention, and high flexibility against changes in pollution and environmental conditions, have been intensively demonstrated.[2] These advantages ensure a high application potential of the AGS technology in wastewater treatment. Nonetheless, efficient start-up and stability of AGS process still remain critical issues.[3]

The extracellular polymeric substance (EPS) is known to affect the granulation process of AGS.[4] The main components proteins (PN) and polysaccharides (PS) of EPS are further found to be important in maintaining the properties of AGS.[5] The granular structure is supported by a backbone mainly composed of PS[1,6] and the PN

may improve AGS granulation and structure integrity due to enhanced surface hydrophobicity and the reduced surface negative charge.[4,7] Apart from PS and PN, alginate-like exopolysaccharides (ALE) successfully extracted from the EPS of AGS developed with synthetic wastewater has been confirmed its function of improving formation of AGS.[8] In addition, the EPSs also contain other components, such as lipids and humic, fulvic, amino acids, etc.[1,4] Their roles in EPS's contribution in the granulation and structural stability of AGS are unknown. Therefore, further investigation on possible contributing components of EPSs in AGS is deemed necessary to resolve critical issues.

Our recent study discovered a significant decrease in tyrosine-like compounds in the EPS extracted from the AGS that disintegrated when it exposed to a low COD/N ratio (=1) medium in a sequencing airlift bioreactor (SABR).[9] The effect of tyrosine has been investigated on formation of biofilm, and mainly focused on L and D-tyrosine. The L-tyrosine was found a precursor to *N*-acyl-tyrosine which is bacteria signaling controlling biofilm formation.[10] On the contrary, Kolodkin-Gal et al.[11] reported that D-amino acids including D-tyrosine could prevent biofilm formation. Mixed effects were also observed in "L" isomers of various amino acids, including L-tyrosine; some promoted while some inhibited biofilm formation.[12] An exploratory study on the role of L-tyrosine in aerobic sludge granulation while maintaining the structure integrity needs to be carried out. Aerobic sludge granulation and stability in a SABR dosed with L-tyrosine and that without L-tyrosine dosing as the control system were tested

in parallel. Close monitoring of the physical, chemical and biological characterization of both AGS granules were performed. Findings from this study would shed light on the role of EPS in the AGS formation and stability.

2. Materials and Methods

2.1 Reactor and operation

Aerobic sludge granulation was conducted in two identical SABRs (100 cm in height and 5 cm in diameter with a working volume of 1.1 L in each reactor). The SABRs were operated in parallel under the same conditions, one serving as the control reactor (Ra) free of L-tyrosine, while the other (Rb) tested the effect of L-tyrosine (Sigma Aldrich, St. Louis, MO, USA) dosed via its influent as a constant rate of 6 mg/L, as adopted from a biofilm formation control study.[11,13] A 2-L/min air flow rate was applied in each reactor, maintaining a superficial up-flow air velocity of 1.2 cm/s.[14] Both reactors had a 2.4-h operation cycle comprised of 6 min feeding, 120 min aeration, 5 min settling, 5 min decanting and 8 min idling. The volumetric exchange ratio of each reactor was set at 50%, corresponding to a hydraulic retention time (HRT) of 4.8 h. Details of the operation strategies are provided in Table A.1 in the Supplementary Information (SI).

2.2 Feeding

Both reactors were inoculated with 2 g/L of activated sludge taken from a local sewage treatment plant in Hong Kong. Synthetic wastewater was prepared by diluting the synthetic stock solution (Table A.2 in SI) with tap water to set the influent COD concentration at a typical level, i.e. 400 mg/L. Acetate, glucose and yeast comprised the source of organics. In order to decrease the COD/N ratio in the influent from 4 (phase I) to 1 (Phase II), ammonium chloride was added from day 60 accordingly, in order to increase the influent ammonium concentration from 100 to 400 mg-N/L in Phase I and II respectively (Table A.3 in SI). The ratio of bicarbonate ($NaHCO_3$) to ammonium-nitrogen (N) in the influent was fixed at 4 to maintain pH at 7.9. The ambient temperature in the laboratory was 23±2 °C.

2.3 Analytical methods

2.3.1 Water quality and sludge physical property analysis

COD was determined following the Standard Methods.[15] Total nitrogen (TN) was measured by using a total organic carbon analyzer (TOC-VCPH, Shimadzu, Japan) equipped with a total nitrogen measurement unit (TNM-1, Shimadzu). A flow injection analyzer (QuikChem 8500, Lachat Instruments) was applied to measure the concentration of ammonium nitrogen while the nitrate and nitrite nitrogen were analyzed by using an ion chromatograph (HIC-20A super, Shimadzu). The physical

properties of granular sludge were characterized with mixed liquid suspended solid (MLSS), mixed liquor volatile suspended solids (MLVSS), sludge volumetric index (SVI), particle size distribution, morphology and structure, cohesion, and specific area. MLSS, MLVSS and SVI were measured every two days according to the Standard Method[15]. The size distribution of sludge was determined with a laser diffraction particle size analyzer (LSI3 320, Beckman Coulter). The sludge micro-structure and morphology were examined with a scanning electron microscope (SEM) (JSM 6300F, JEOL) after fixing the sludge sample over night at 4ºC in 2% paraformaldehyde, 2% glutaraldehyde, and 1X phosphate-buffered saline (PBS) mixed solution and subsequent lyophilization. Cohesion tests followed the protocol reported by Wan et al.[16] with the following modifications: 1) measurement chamber geometry: closed with a volume of 520 mL, diameter 100 mm, depth 66 mm, paddle diameter 63 mm, and paddle height 24 mm placed at 1/3 of the chamber height from the bottom (paddle power number Np of 2.9), and 2) a series of velocity gradients of 250, 13230 and 250 s^{-1} were applied. The specific area and total pore volume of sludge were also examined by using an automatic instrument (ASAP 2020, Micrometrics) and then determined from the Brunauer–Emmett–Teller (BET) method.[17]

2.3.2 EPS analysis

EPS content and component

EPS was first extracted from the sludge using a formaldehyde-NaOH method.[18] The carbohydrate or polysaccharide (PS) in EPS was then quantified by using the phenol-sulfuric acid (PSA) method with glucose as the standard.[19] The protein (PN) in EPS was determined from the modified Lowry colorimetric method with bovine albumin serum as the standard.[20] A luminescence spectrometer (F-4500 FL Spectrophotometer, Hitachi) was used to examine the EEM spectra of extracted EPS for components identification with methodology applied as previously described[9].

2.3.3 Microbial diversity analysis

A Power Soil DNA extraction kit (MO BIO Laboratories Inc.) was periodically applied to extract DNA from the sludge samples taken from both reactors. The 16S rDNA gene was amplified by PCR with the following steps: 94 ºC for 5 min followed by 30 cycles of 94 ºC for 30 s, 53 ºC for 30 s and 72 ºC for 45 s; and a final extension at 72 ºC for 10 min. Then 200ng of purified 16S rDNA amplicons from each sample were pooled and subjected to pyrosequencing using the ROCHE 454 FLX Titanium platform (Roche) at the National Human Genome Centre of China in Shanghai, China. The pyrosequencing methodology employed was the same as previously described[9].

Low quality sequences were removed from raw sequence data by trimming the barcode tags and primer sequences. FASTA files were generated from the resulting sequences according to the barcodes of individual samples. The sequences were then

aligned using the software Mothur ver. 1.17.0[21] and the distance matrix was produced. Operational taxonomic units (OTU) were determined at 90, 95 and 97% similarities (Mothur v. 1.17.0). Rarefaction curves and diversity indices (ACE and Chao1) were determined from the calculated OTUs using the same software. In the taxonomy-based analysis, the representative sequences from each OTU were subjected to the RDP-II Classifier of the Ribosomal Database Project (RDP),[22] the National Centre for Biotechnology Information (NCBI) BLAST,[23] and the Greengenes Databases.[24] The relative abundance and occurrence of the tags assigned into these three samples were visualized as a heat map using the Multi Experiment Viewer (MeV) v4.8.1 software.

3. Results

3.1 Formation of aerobic granules

Disintegration of AGS induced by low COD/N ratio (i.e., COD/N = 1) has been confirmed in our previous work[9]. Thus, to eliminate unexpected effects imposed by factors other from the L-tyrosine, both reactors were started up under an appropriate COD/N ratio of 4 in the formation phase (phase I). The seeding sludge was aerated for 2 days in both reactors prior to the inoculation. A short settling time (5 min) was then applied in both reactors. MLSS was intensively monitored during the start-up period. In the control reactor, a decrease of MLSS was observed within the first 18 days

(from 2 to 1.4 g/L), but the sludge in the test reactor showed excellent settling properties, enabling a continuous increase in MLSS from initially 2 to 6.4 g/L at day 76 (see Fig. 1a).

Figure 1b shows the mean particle diameter of the sludge in each reactor. The mean particle size in the test reactor reached 200 μm after 7 days and then became stable at 2,150 ± 20 μm after 32 days. The SVI_5 of both reactors was initially 100 mL/g. After 11 days' operation, SVI_5 of the test reactor significantly decreased to 35 mL/g and subsequently remained at around 47 mL/g throughout the entire period. Conversely, the SVI_5 of the control reactor stayed unchanged until day 39, and then gradually reduced to 76 mL/g after day 46. Apparently, granulation in the control reactor was much slower than that in the test reactor, though its sludge floc size was measured to be 200 μm or above from day 14. The ratio of SVI_5 to SVI_{30} is often used to evaluate the extent of granulation, and when the value is close to unity full granulation is recognized.[25] Figure 1c illustrates that the ratio of SVI5/SVI30 was close to unity in the test reactor after 11 days, and 39 days were required for the control reactor, i.e. 28 days longer than the test reactor.

3.2 Stability of aerobic granular sludge

In our previous stability study of AGS, the granules underwent a condition of stepwise decrease in COD/N ratio from 4 to 1, and eventually disintegration occurred

at a ratio of 1.[9] Accordingly, after full granulation was achieved in these two reactors, the COD/N ratio was decreased from 4 at day 60 to 1 at day 120 to investigate the effect of L-tyrosine on the stability of aerobic granules, during which the key physical, chemical and biological characteristics of both AGSs were monitored closely. The respective results are summarized below.

3.2.1 Particle size and settling ability

With a decrease of COD/N ratio from 4 to 1, the mean diameter of the granules in the test reactor remained stable at 2100±100μm throughout the operation, and in the control reactor significantly decreased by 90% from 1600±50 μm initially to 200 ±18μm after 60 days (see Fig. 2a).

Meanwhile, the SVI_5 of the control reactor increased from 55±5 mL/g to 110 ±10 mL/g. However, that of the test reactor maintained at 50 ±5 mL/g till the end of the experiment. According to the ratio of SVI_5/SVI_{30}, AGS in the control reactor disintegrated after day 88, while the test reactor maintained the extent of granulation during the whole operation in Phase II with COD/N equal to 1 (see Fig. 2b). Due to the deterioration of the settling ability of AGS in the control reactor, half of the sludge was washed out, i.e. the MLSS concentration decreased from 6 g/L at day 94 to 3 g/L at the end of the experiment. Comparatively, the MLSS in the test reactor increased from 5.9 to 7.6 g/L (see Fig. 2c).

223

224 3.2.2 Performance of the reactors

225

226 The ammonium nitrogen removal efficiencies of both reactors during the entire
227 operation are shown in Fig. 3. Both reactors showed similar removal efficiency (more
228 than 90%) during the granulation period (Phase I, COD/N=4). With the COD/N ratio
229 further decreased from 4 to 1, the removal efficiency of both reactors was halved at
230 day 60. The removal efficiency of the control reactor continually decreased to 17%
231 eventually. Conversely, that of the test reactor gradually recovered to 75% at the end
232 of experiment.

233

234 The maximum oxidation rate of the ammonium and nitrite in both reactors in Phases I
235 (COD/N=4) and II (COD/N=1) were determined from the cycle tests conducted with
236 a dissolved oxygen (DO) concentration fixed at 8.2 mg/L. As shown in Table 1, the
237 rates of the test reactor were determined to be 8.4 and 3.0 mg N/g VSS·h, 50 and 43%
238 higher than that of the control reactor (5.6 and 2.1 mg N/g VSS·h) in Phase I
239 (COD/N=4). The maximum oxidation rate of ammonia increased to 19.4 in the
240 control reactor and 21.8 mg N/g VSS·h in the test reactor while the ratio of COD/N
241 decreased to 1 in Phase II. The nitrite oxidation rate in the test reactor maintained at
242 2.9 mg N/g-VSS·h, but in the control reactor, it increased threefold to 6.1 mg
243 N/g-VSS-h due to the disintegration of AGS in control reactor after the COD/N ratio
244 decreasing to 1.

In phase I, TN loss in the control reactor (35±5%) was greater than that (30±5%) in the test reactor (see Fig. 3b), which could be ascribed to higher porosity of AGS in the testing reactor (Table 2) decreasing anaerobic zones in granules. When the COD/N ratio decreased from 4 to 1, the TN loss gradually reduced in this reactor due to disintegration of granules, however the TN loss in the test reactor still remained at between 20 and 30% when the ratio reached 1, with the stable porosity and surface area features of AGS maintained (see Table 2). The reasons for such stable properties of the granules is further discussed in Section 3.2.3. The COD removal efficiency of both reactors was maintained at more than 85% throughout the operation.

3.2.3 Physical characteristics of granules

The physical strength of the granules in both reactors was measured to illustrate their structural features and capability to withstand high abrasion and water shear forces. Figure 4 shows the cohesion results of the granules in both reactors. During Phase I (COD/N=4), no apparent coagulation and break-up of the granules were observed in the control reactor when the mixing forces (G value) was $250s^{-1}$, 13230 s^{-1} and 250 s^{-1} successively. This confirmed that the sludge in this reactor was of pure granular structure.[16] However, when the same G-values were applied to the test reactor, break-up and re-coagulation were observed (see Fig.4a) though the granules remained intact, indicating that flocculent sludge-like properties were incorporated in the granules in the test reactor. The same sludge behavior in the test reactor was observed

in Phase II (COD/N=1), with a complete dispersion occurring in the control reactor (see Fig. 4b).

The physical strength of the granules is usually negatively correlated with its porosity,[26] which determines substrate transport and oxygen diffusion within the granules. Hence the porosities of the granules in both reactors under different COD/N ratios were examined, as shown in Table 2. With the COD/N ratio decreased from 4 to 1, the surface area (BET) and total pore volume of the granules in the control reactor clearly rose from 1.9 to 4.5 m^2/g and 9.0 to 18.1 ml/kg-VSS respectively, in line with the results of the cohesion tests. Accordingly, the surface area and total pore volume of the granules in the test reactor were maintained at 3.5 m^2/g and 13.0 ml/kg-VSS, respectively.

4. Discussion

4.1 Effect of L-tyrosine on formation and stability of AGS

The production of EPSs, especially the PS and PN compounds, plays a key role in aerobic granulation and structure integrity via altering the physical-chemical properties of the cellular surface of AGS, such as hydrophobicity and charge.[5,27] The change of certain components in EPSs, e.g., tyrosine-like compounds fading out in the disintegrating AGS was revealed by Luo et al.[9] In the present study, the effect of L-tyrosine on AGS is to: accelerate granulation (stage I) with L-tyrosine at 6 mg/L,

acquiring AGS formation within 11 days, i.e. 5 days shorter than the fastest granulation period ever reported (see Table 3) and a stable reactor performance as well as structural integrity of AGS in terms of the changes in diameter and physical strength (Phase II).

4.2 The production of EPS

As shown in Figure 5, in Phase I (COD/N=4), the PS content of the granules in the test reactor reached 38 mg/ g-VSS, two times greater than that in the control reactor. When the COD/N ratio reduced to 1 at day 60, the PS extracted from the granules in the test reactor slightly decreased to 35 mg/g-VSS; comparatively it significantly decreased by 50% to 10 mg/g-VSS in the control reactor, which in turn disintegrated the granules (Fig. 2). This indicated the importance of EPS in stability maintenance of the AGS. Stable secretion of EPS in test reactor can be ascribed to three reasons. Firstly, the porous structure of the L-tyrosine-promoted granules. Higher porosity of the aerobic granules in the test reactor could relieve the limitation of mass transfer and thus maintained PS secretion in the center of the granules.[1,4] Secondly, the L-tyrosine as substrate can be utilized by bacteria to synthesize *N*-acyl-tyrosine which promotes the production of EPS[10]. Thirdly, the L-tyrosine is the main compound of the tyrosine kinase and tyrosine phosphatases which are vital to cell regulatory enzymes for a number of microbial processes, including EPS secretion.[32]

313 At the end of experiment, a 3D-EEM analysis was conducted to identify the different
314 tyrosine-EPS in both reactors. The results indicate that the tyrosine protein-like
315 (region A) substances were observed in granules of both reactors in phase I.
316 Subsequently the tyrosine protein-like contours faded out in the granules of the
317 control reactor after the COD/N ratio decreasing from 4 to 1, but can be detected in
318 the testing reactor throughout the reactor operation (see Fig. A.1 in SI). In our
319 pervious study, the tyrosine protein-like compound in EPS correlated with the
320 disintegration of aerobic granules under extremely low COD/N ratio. Therefore, the
321 accumulation of tyrosine protein-like would be one of the reasons for the integrity
322 structure of aerobic granules in testing reactor under phase II.
323
324 4.3 The improvement of microbial community
325
326 The microbial communities of the granules in both reactors were analyzed and
327 compared by 16S rDNA pyrosequencing at the end of the experiment. Approximately
328 40,000 and 50,000 effective sequence tags were retrieved from the two types of
329 granules (control and L-tyrosine-promoted). Sufficient sequencing was confirmed by
330 the rarefaction curves (see Fig. A.2 in SI).
331
332 At the phylum level, proteobacteria in L-tyrosine-promoted granules accounted for 80%
333 much higher than the control granules (57%). This phylum is reported to associate
334 with the production of *N*-acyl-tyrosine which can promote production of EPS[10]. The

abundance of bacteroidetes (27%), which are responsible for secreting lectin-specific EPS (glycoconjugates) for cell attachment,[33] was 3.5 times higher in the L-tyrosine-promoted granules than in the control granules (8%).

At the genus level (Fig. 6), the abundance of *Flavobacterium* (3.3%), *Nitrosomonas* (3.0%) and *Thauera* (15%) in the L-tyrosine-promoted granules were much higher than those of the control granules (0.2, 1.6 and 0.7%, respectively). Meanwhile, all of the aforesaid genera have been shown to contain species that positively correlate with the quorum sensing (QS) auto-inducers during granulation.[34] The QS auto-inducers, especially *N*-acyl-homoserine-lactone (AHL), have been recently recognized as signaling molecules for biofilm development.[34] These genera could be driving or accelerating the granulation when L-tyrosine dosed. In addition, chemical similarities between AHL and *N*-acyl-tyrosine has been reported previously[10] and they both can enhance the formation of biofilm. However connections between L-tyrosine, AHL and these genera are not clear yet, and a further study is deserved.

The portion of Flavihumibacter was larger in the L-tyrosine-promoted granules (1.9 %) than the control granules (0.1 %). Flavihumibacter belongs to filamentous bacteria which can accelerate aerobic granulation with high porosity by offering a structural network to aggregate the cells together.[35] Therefore, the richness of Flavihumibacter with L-tyrosine dosing could be another cause for the high porosity of AGS in the test reactor.

AOB *Nitrosomonas* in the L-tyrosine-promoted and control granules accounted for 3 and 1.5 % respectively. NOB *Nitrospira* and *Nitrobacter* were rare in both granules (< 0.3%), and such low abundance of NOB reflects the accumulation of nitrite in both reactors. The minimum sludge retention times (SRTs) were calculated for both AOB and NOB, as shown in Table A.5 in SI. The mean SRT of both reactors was 8 days longer than the minimum SRT for AOB and NOB, i.e. 4.4 and 1.8 days. Tarre et al., (2007) indicated an optimum pH range for AOB and NOB growth of 7.0 to 8.5 and 7.3 to 7.5, respectively. The low NOB abundance is most likely caused by the influent pH of 7.5-8.0 in the reactors. Additionally, the highly porous structure of L-tyrosine-promoted granules is beneficial to the development of AOB abundance from which oxygen can easily penetrate into core area of the granules.

5. Conclusions

With dosing of L-tyrosine, test reactor achieved full granulation after 11 days' operation, and maintained structural integrity when decreased COD/N ratio from 4 to 1. Granules in test reactor were determined more porous than that in the control reactor, and this property potentially mitigates the mass transfer limitation in the granules. The stable secretion of EPS and the enrichment of genera related to the secretion of QS auto-inducers and filamentous in the test reactor were suggested as the main reasons for the positive effect of tyrosine on the granulation and stability of

AGS.

Acknowledgement

This work is partly supported by China Natural Science Foundation (38000-41030553).

Reference

1. S. S. Adav, D. J. Lee, *Journal of Hazardous Materials*, 2008, **154**, 1120-1126.
2. M. K. de Kreuk, N. Kishida, M. C. M. van Loosdrecht, *Water Science & Technology*, 2007, **55**, 75-81.
3. K. Y. Show, D. J. Lee, J. H. Tay, *Applied Biochemistry and Biotechnology*, 2012, **167**, 1622-1640.
4. B. S. McSwain, R. L. Irvine, M. Hausner, P. A. Wilderer, *Applied and Environmental Microbiology*, 2005, **71**, 1051–1057.
5. J. E. Schmidt, B. K. Ahring, *Applied Microbiology and Biotechnology*, 1994, **42**, 457–62.
6. B. Long, C. Z. Yang, W. H. Pu, J. K. Yang, Y. F. Shi, J. Wang, J. Bai, X. Y. Zhou, G. S. Jiang, C. Y. Li, F. B. Li, *Bioresource Technology*, 2014, **169**, 244-250.
7. L. Zhu, M. L. Lv, X. Dai, Y. W. Yu, H. Y. Qi, X. Y. Xu, *Bioresource Technology*, 2012, **107**, 46-54.
8. Y. M. Lin, M. de Kreuk, M. C. M. van Loosdrecht, A. Adin, *Water Research*, 2010. **44**, 3355-3364.
9. J. H. Luo, T. W. Hao, L. Wei, H. R. Mackey, Z. Q. Lin, G. H. Chen, *Water Research*, 2014, **62**, 127-135.
10. J. W. Craig, M. A. Cherry, S. F. Brady, *Journal of Bacteriology*, 2011, **193**, 5707-5715.
11. I. Kolodkin-Gal, D. Romero, S. Cao, J. Clardy, R. Kolter, R. Losick, *Science*, 2010, **328**, 627-629.
12. S.N. Goh, A. Fernandez, S.Z. Ang, W.Y. Lau, D.L. Ng, E.S.G. Cheah, *Journal of Biology and Life Science*, 2013, **4**, 103-115.
13. H. J. Xu, Y. Liu, *Water Research*, 2011, **45**, 5796-5804.
14. J. H. Tay, Q. S. Liu, Y. Liu, *Water Science and Technology*, 2004, 49, 35–40.
15. APHA, AWWA, WEF, 21st ed, Washington, D.C. 2005.
16. J. F. Wan, I. Mozo, A. Filali, A. Line, Y. Bessiere, M. Sperandio, *Biochemical Engineering Journal*, 2011, 58–59, 69–78.
17. V. Fierro, F. V. Torne, D. Montane, A. Celzard, *Microporous and Mesoporous Materials*, 2008, **111**, 276–284.
18. H. Liu, H. H. Fang, *Journal of Biotechnology*, 2002, **95**, 249-56.
19. M. Dubois, K. A. Gilles, J. K. Hamilton, P. A. Rebers, F. Smith, *Analytical Chemistry*, 1956, **28**, 350-356.
20. B. Frølund, T. Griebe, P. H. Nielsen, *Applied Microbiology and Biotechnology*, 1995, **43**, 755-761.
21. P. D. Schloss, S. L. Westcott, T. Ryabin, J. R. Hall, M. Hartmann, E. B. Hollister, R. A. Lesniewski, B. B. Oakley, D. H. Parks, C. J. Robinson, J. W. Sahl, B. Stres, G. G. Thallinger, D. J. van Horn, C. F. Weber, *Applied and Environmental Microbiology*, 2009, **75**, 7537–41.
22. J. R. Cole, Q. Wang, E. Cardenas, J. Fish, B. Chai, R. J. Farris, A. S. Kulam-Syed-Mohideen, D. M. McGarrell, T. Marsh, G. M. Garrity, J. M. Tiedje, *Nucleic Acids Research*, 2009, **37**, 141–145.

23. M. Johnson, I. Zaretskaya, Y. Raytselis, Y. Merezhuk, S. McGinnis, T. L. Madden, *Nucleic Acids Research*, 2008, **36**, W5–W9.
24. T. Z. de Santis, P. Hugenholtz, N. Larsen, M. Rojas, E. L. Brodie, K. Keller, T. Huber, D. Dalevi, P. Hu, G. L. Andersen, *Applied and Environmental Microbiology*, 2006, **72**, 5069–5072.
25. M. K. de Kreuk, J. J. Heijnen, M. C. M. van Loosdrecht, *Biotechnology and Bioengineering*, 2005, **90**, 761-9.
26. R. Lemaire, R.I. Webb, Z. G. Yuan, *ISME Journal*, 2008, **2**, 528–541.
27. Y. Liu, S. Y. Yang, J. H. Tay, Q. S. Liu, L. Qin, Y. Li, *Enzyme and Microbial Technology*, 2004, **34**, 371–379.
28. X. H. Wang, M. H. Diao, Y. Yang, Y. J. Shi, M. M. Gao, S. G. Wang, *Bioresource technology*, 2012, **110**, 105-110.
29. M. Pijuan, U. Werner, Z. G. Yuan, *Water Research*, 2011, **45**, 5075-5083.
30. L. Liu, D. W. Gao, Min. Zhang, F. Yuan, *Journal of Hazardous Materials*, 2010, **181**, 382-387.
31. X. M. Li, Q. Q. Liu, Q. Yang, L. Gao, G. M. Zeng, J. M. Hu, W. Zheng, *Bioresource Technology*, 2009, **100**, 64-67.
32. A. J. Standish, A. A. Salim, H. Zhang, R. J. Capon, R. Morona, *PLoS ONE*, 2012, **7**, 5.
33. M. B. Chiristin, R. N. Thomas, M. F. Bernhard, A. Rudolf, *Systematic and Applied Microbiology*, 2013, **36**, 417-425.
34. C. H. Tan, K. S. Koh, C. Xie, M. Tay, Y. Zhou, R. Williams, W. J. Ng, S. A. Rice, S. Kjelleberg, *ISME Journal*, 2014, **8**, 1186-97
35. Y. M. Zheng, H. Q. Yu, S. J. Liu, *Chemosphere*, 2006, **63**, 1791–1800.

LIST OF TABLES AND FIGURES

TABLES

FIGURES

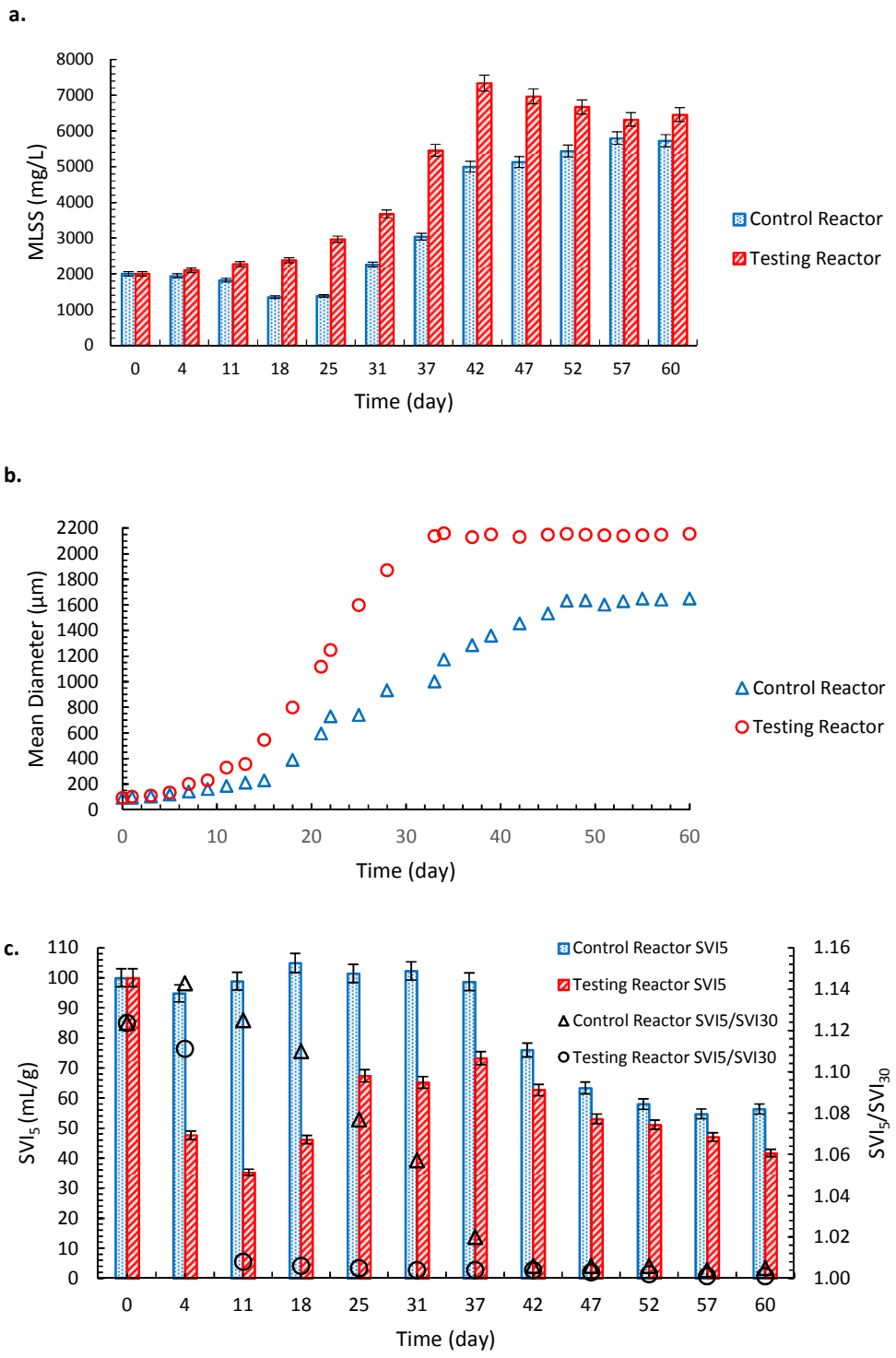

Fig. 1 Profile of sludge indices under granulation period (Phase I) with COD/N ratio of 4 for: (a) MLSS, (b) mean diameter of granules, and (c) SVI_5 and SVI_5/SVI_{30}

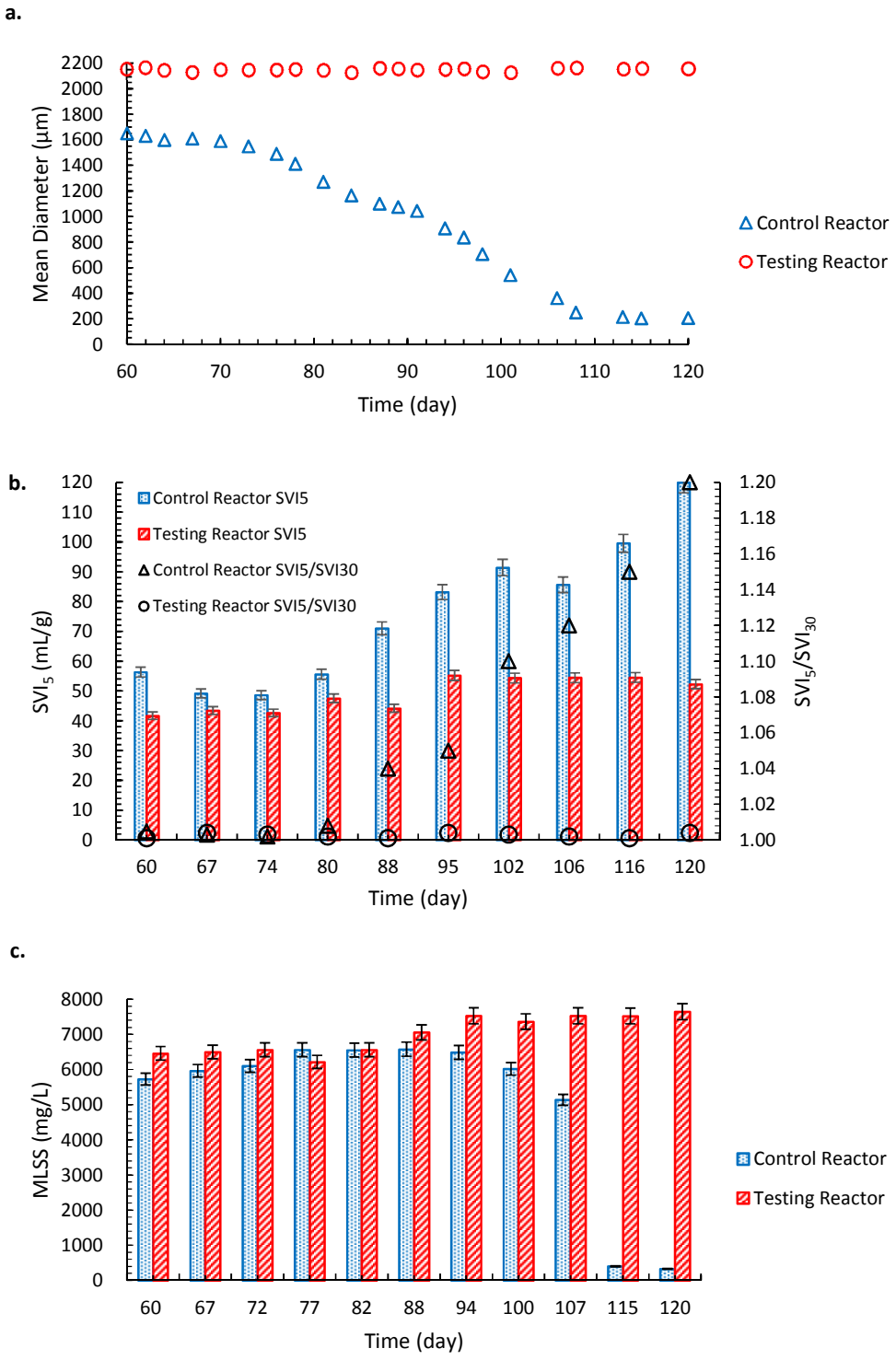

Fig. 2 Profile of sludge indices in Phase II with COD/N =1: (a) mean diameter of granules, (b) SVI_5 and SVI_5/SVI_{30}, and (c) MLSS

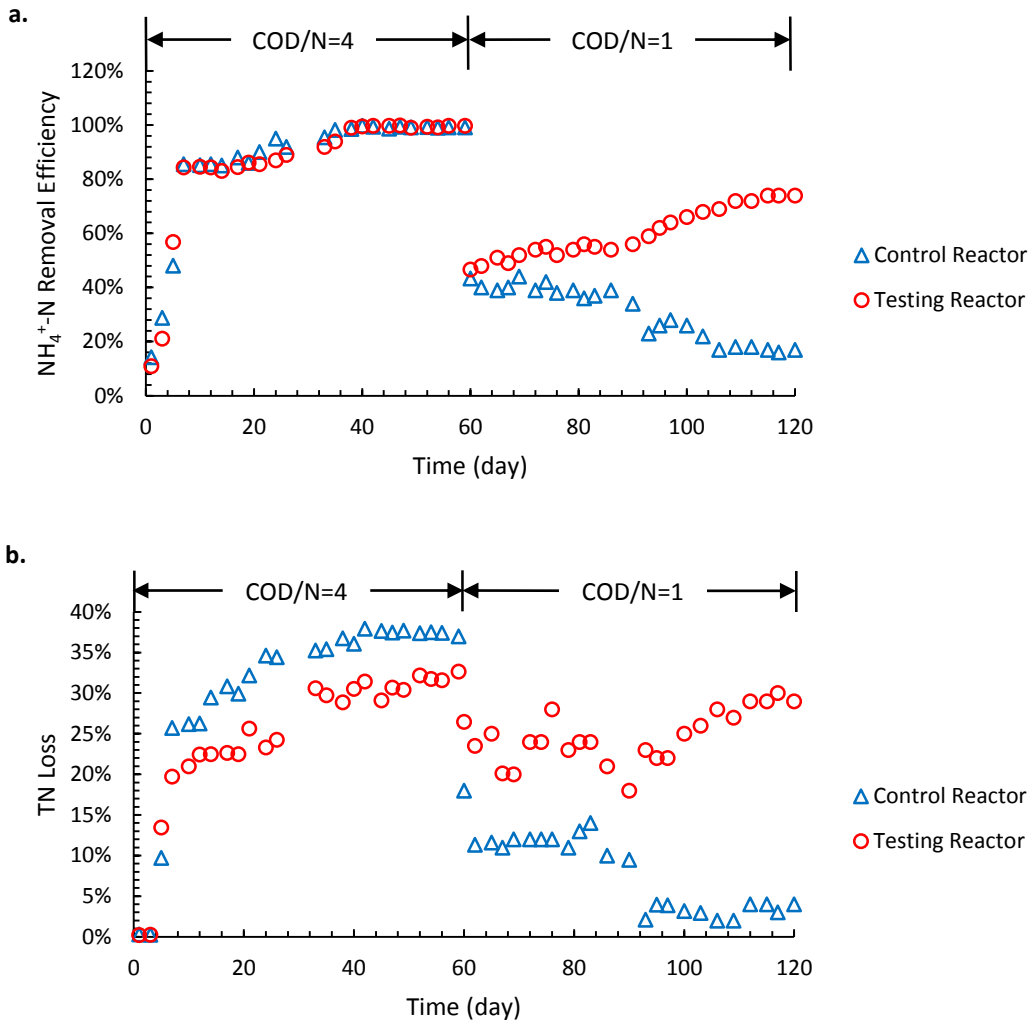

Fig. 3 Profile of the removal efficiencies in both reactors during the whole operation for (a) ammonia and (b) TN

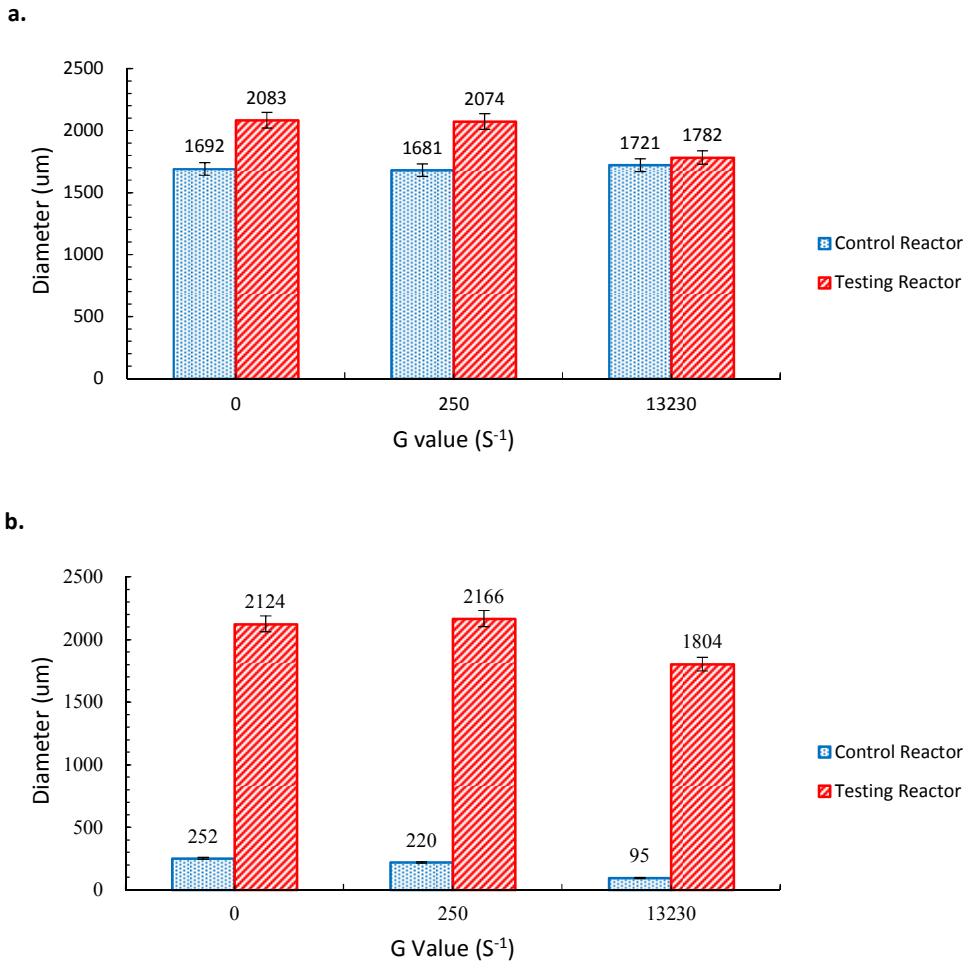

Fig. 4 Changes in the mean particle size of the granular sludge during the cohesion tests: (a) Phase I (COD/N=4), (b) Phase II (COD/N=1)

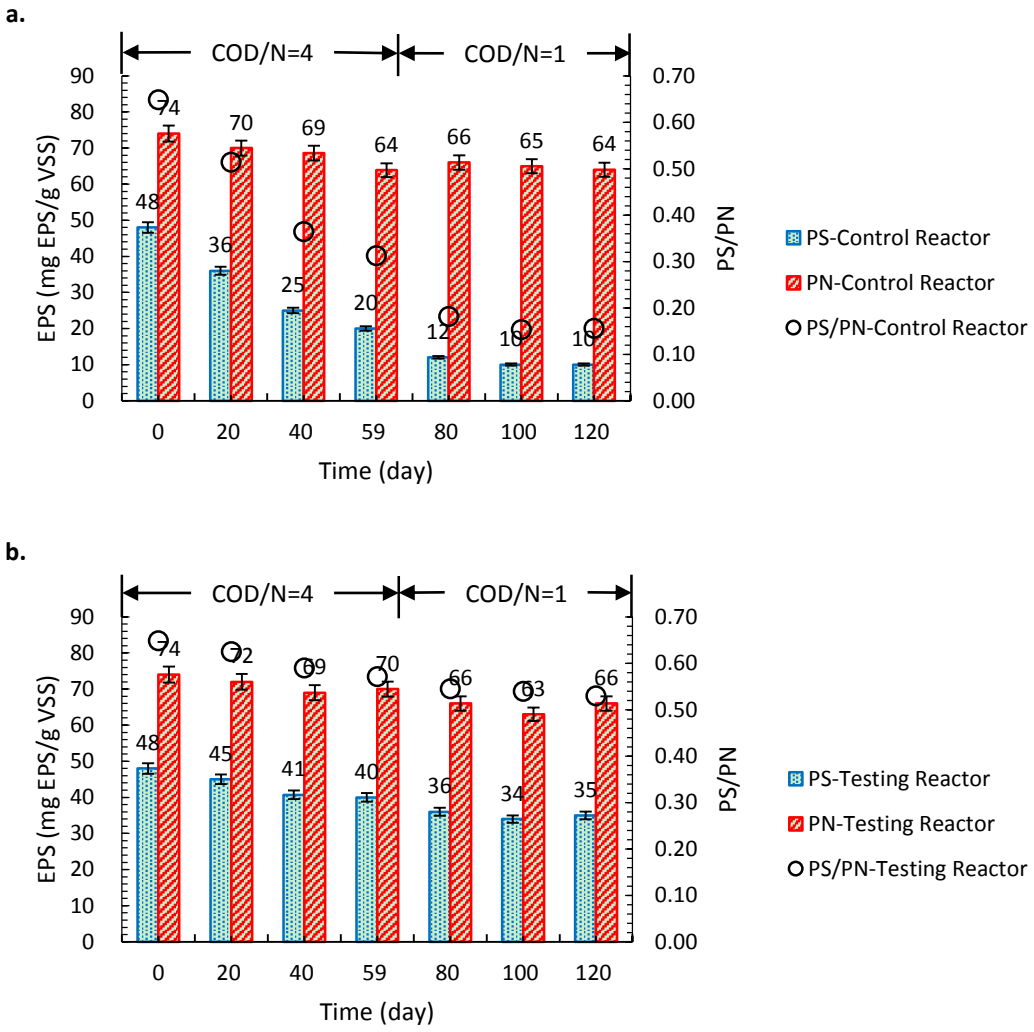

Fig. 5 Profiles of EPS content of the granular sludge in (a) control reactor, (b) testing reactor

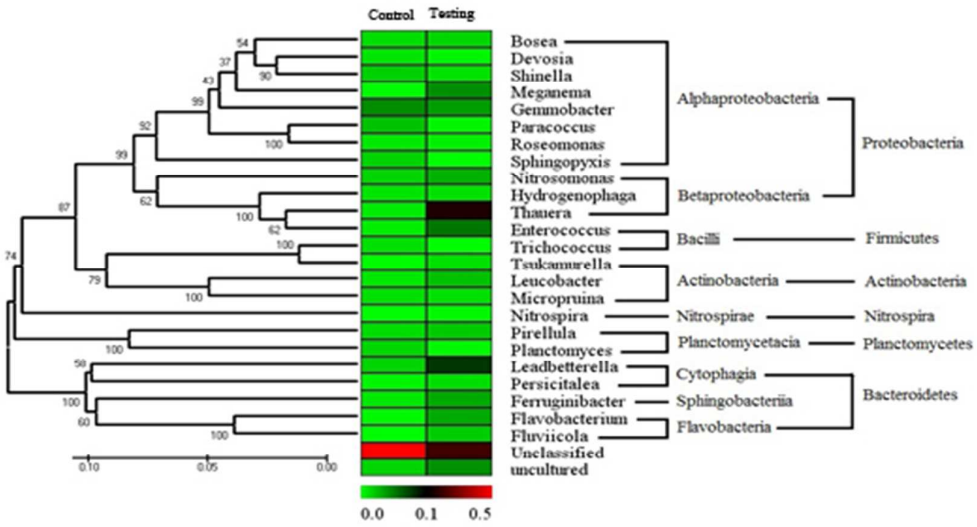

Fig. 6. Taxonomic classification of bacterial 16s rDNA reads retrieved from sludge of the control and testing reactors at genera level

Table 1. Maximum oxidation rates (mg N/g VSS·h) of ammonium and nitrite

	Phase I, COD/N=4		Phase II, COD/N=1	
	Control Reactor	Testing Reactor	Control Reactor	Testing Reactor
Max. NH_4^+ oxidation rate	5.6 ± 0.2	8.4 ± 0.3	19.4 ± 0.5	21.8 ± 0.5
Max. NO_2^- oxidation rate	2.1 ± 0.1	3.0 ± 0.2	6.1 ± 0.2	2.9 ± 0.1

Table 2. Surface area and porosity of granules in phases I and II

COD/N	BET Surface Area (m^2/g)		Total Pore Volume (ml/kg-VSS)	
	Control Reactor	Testing Reactor	Control Reactor	Testing Reactor
4	1.9±0.2	3.6±0.4	9.0±0.6	13.4±1.2
1	4.5±0.4	3.4±0.3	18.1±1.1	12.6±0.9

Table 3. AGS granulation time vs different enhancing methods

Strategies	granulation period (days)	References
Static magnetic field	25	28
50% crashed granules mixed	20	29
Ca^{2+} augmentation	17	30
Mg^{2+} augmentation	16	31
L-tyrosine	11	Present study